JACS
JOURNAL OF THE AMERICAN CHEMICAL SOCIETY

Communication

pubs.acs.org/JACS

Magnetic Dipolar Interactions in Solid Gold Nanosphere Dimers

Manabendra Chandra, Anne-Marie Dowgiallo, and Kenneth L. Knappenberger, Jr.*

Department of Chemistry and Biochemistry, Florida State University, Tallahassee, Florida 32306-4390, United States

Supporting Information

ABSTRACT: We report the first observation of a magnetic dipolar contribution to the nonlinear optical (NLO) response of colloidal metal nanostructures. Second-order NLO responses from several individual solid gold nanosphere (SGN) dimers, which we prepared by a bottom-up approach, were examined using polarization-resolved second harmonic generation (SHG) spectroscopy at the single-particle level. Unambiguous circular dichroism in the SH signal was observed for most of the dimeric colloids, indicating that the plasmon field located within the interparticle gap was chiral. Detailed analysis of the polarization line shapes of the SH intensities obtained by continuous polarization variation suggested that the effect resulted from strong magnetic-dipole contributions to the nanostructure's optical properties.

Plasmon-supporting metal nanostructures have been studied extensively in recent years both as isolated systems and as arrays.[1] Much of this work has focused on the surface plasmon resonance (SPR) of these nanostructures, which enhances the effects of electromagnetic fields in close proximity to the nanostructure surface. In a phenomenon known as the lighting rod effect, electromagnetic fields become focused in the small volumes constituting the interparticle gaps of nearby nanoparticles, thus magnifying the strength of the field.[2,3] These enhancements have been used to improve nanoparticle-assisted biosensing and applied spectroscopy.[4−14] In the case of surface-enhanced Raman scattering, plasmonic structures with complex shapes have been tailored for optimal performance.[9−12] Plasmonic nanostructures have also been incorporated into solar cells to enhance light absorption.[13,14] In light of the growing exploitations of field-enhancement phenomena in composite metal nanostructures, a predictive understanding of the interplay between the nanoscale structure and the optical properties is necessary.

Among other theoretical models, plasmon hybridization,[15] transformation optics,[16] and plasmon-ruler relations[17] have been used to explain the (magnitude and) frequency of the SPR arising from electromagnetic coupling between metal nanostructures. These models allow for both a detailed physical understanding of the fabricated structures and the prediction of many effects for dimers,[17] quadrumers,[18] and oligomers.[19] Experimental data obtained using linear optical techniques such as dark-field and Rayleigh scattering are also consistent with the predicted resonance frequencies provided by these models.[20] However, the properties of the electromagnetic fields that result from interparticle interactions are still not well understood. To provide detailed structure-specific descriptions of these interfacial fields, an optical technique is needed that is both highly sensitive to the interparticle electromagnetic fields and able to be used at the single-particle level. The latter criterion stems from the inherent sample polydispersity of colloidal metal nanoparticles, which would obscure structure−property relationships in ensemble measurements. Nonlinear optical (NLO) techniques satisfy both of these requirements: they are highly sensitive to local fields,[21] and because NLO processes involve energy up-conversion, they provide higher spatial resolution for single-particle measurements. The high field sensitivity arises because the induced polarization, which radiates at the wave-mixing frequency, is a nonlinear function of the optical field: for an nth-order NLO process, the nonlinear radiation intensity is proportional to the $(2n)$th power of the field. This high field sensitivity means that NLO spectroscopic/microscopic techniques can report on local electromagnetic fields in interacting plasmonic nanostructures.

Second harmonic generation (SHG) is a second-order interface-sensitive NLO process[22−29] that is well-suited for studying the properties of electromagnetic fields localized at the interface of metal nanostructures. As such, SHG is ideal for gaining insight into nanostructure morphology and symmetry and the resulting optical properties. The use of SHG in this manner has been demonstrated on chiral planar metal nanostructure arrays that were fabricated using top-down lithographic techniques.[22−27] In these studies, a distinct circular dichroism (CD) was noted in the SHG intensities observed for nanostructures with known chiral symmetry. By comparison, the structural heterogeneity within samples generated via bottom-up assembly makes a priori knowledge of the metal nanostructure's symmetry and corresponding electromagnetic field difficult. Nonetheless, the bottom-up approach offers significant advantages. First, through surface functionalization methods, plasmon-supporting nanostructures can be arranged with spatial separations ranging from less than 1 nm to several nanometers; this span encompasses the zone containing the transition from conductively overlapping to dielectrically screened nanoparticles. As a result, colloidal wet-chemistry methods can be used to tailor in-plane plasmon hybridization.[30] Furthermore, the use of this length scale allows for systematic tuning of the coupling mechanism, a significant advantage for photonic and plasmonic applications. The inherent synthetic flexibility of bottom-up assembly permits the design of materials with controlled electric, magnetic, and Fano-like interactions. Taken together, the repertoire of systems available through bottom-up syntheses and the structure-specific and field-sensitive nature of SHG can be used to develop a predictive understanding of colloidal structure−property relationships.

Received: November 12, 2011
Published: February 29, 2012

dx.doi.org/10.1021/ja210648a | J. Am. Chem. Soc. 2012, 134, 4477−4480

Here we demonstrate continuous polarization variation SHG (CPV-SHG) measurements on single solid gold nanosphere (SGN) dimers, with these data being assigned to specific structures that were identified via electron microscopy. We observed unambiguous CD in the SHG of several SGN dimers. Thorough analysis of the complete polarization-resolved NLO response (i.e., rotation over 360°) revealed that the observed chirality was in fact the result of both electric-dipole and strong magnetic-dipole contributions to the sample's nonlinear susceptibility. To our knowledge, this is the first experimental confirmation of magnetic-dipole contributions to the NLO response of electromagnetically coupled colloidal nanoparticles.

The samples consisted of SGN dimers drop-cast onto an indexed patterned glass coverslip. The SGNs were synthesized by a standard citrate reduction method[31] [for synthesis and sample preparation details, see the Supporting Information (SI)]. Small aggregates were formed by the introduction of a controlled quantity of aqueous cysteine solution (see the SI). Although this synthetic approach does not form dimers exclusively, optical and electron microscopy permitted selective study of only these aggregates for the current work. Nanosphere dimers consisting of monomers joined together via cysteine linkages are characterized by an interparticle gap of ∼1.2 nm.[32] Upon laser excitation, electromagnetic fields are localized in this gap, resulting in the SHG-signal-inducing polarizability.

The experimental setup used for single-structure SH microscopy is depicted in Figure S3 in the SI. The nonlinear excitation source was a mode-locked Ti:sapphire laser (Mantis, Coherent Inc.), which delivered 65 fs pulses at a 54 MHz repetition rate. The fundamental output of the laser was centered at 800 nm and focused onto the sample by an aspheric lens [numerical aperture (NA) = 0.5], leading to a focal spot diameter of ∼1 μm. The sample plane was mounted normal to the laser propagation direction. Typical excitation laser pulse energies were ∼30 pJ/pulse. The polarization state of the exciting laser beam was controllably varied from linear to elliptical to circular by using a rotating quarter-wave plate (QWP). The SHG signal was collected in the transmission direction using a high-NA (1.25) oil-immersion objective. The fundamental light was rejected using a dichroic mirror and a series of short-pass filters (HQ 680-SP, Chroma Technology). A polarizer was used in the detection arm for CPV-SHG measurements. The SH light was isolated using a band-pass filter centered at 400 nm (HQ 400/20 m-2P, Chroma Technology) and focused to a photomultiplier tube (PMT) (R7205-01, Hamamatsu) operated in photon-counting mode. The output from the PMT was monitored using a single-photon counting unit (Becker & Hickl). The home-built optical microscope also included bright-field capability, which was used to determine the exact coordinates of the segment of the patterned coverslip that was in the focal volume during each SHG measurement. These registry markings were then used to locate the nanostructures for electron microscopy measurements, allowing the optical properties to be correlated to structure.

We first consider the differential CD in the SHG signal from a SGN dimer. Differential CD in SHG is the difference in the SH intensities obtained from a sample upon excitation with left circularly polarized (LCP) and right circularly polarized (RCP) light. Differential CD is quantified by a normalized quantity termed the SHG circular difference ratio (SHG-CDR), which is typically used to express the extent of chirality of a structure; this ratio is given by

$$\text{SHG-CDR} = \frac{2(I_{2\omega}^{\text{LCP}} - I_{2\omega}^{\text{RCP}})}{I_{2\omega}^{\text{LCP}} + I_{2\omega}^{\text{RCP}}} \quad (1)$$

where $I_{2\omega}$ is the experimentally measured SHG intensity. It is evident from eq 1 that the SHG-CDR can have any value between 0 and 2 (or 0% and 200%). Figure 1a shows the SH intensity resulting from excitation of an SGN dimer by LCP and RCP light. A large and unambiguous difference in the SH response was observed for the two different excitation polarization states, demonstrating the chirality of the dimer structure. The corresponding SHG-CDR was measured to be 1.1 (110%). SHG-CDR data were collected for several SGN dimers, most of which exhibited SH optical activity (Figure 1b). However, the magnitude and sign of the SHG-CDR fluctuated significantly among dimers, indicating that the differential CD response is highly structure-specific. The variation among the SHG-CDRs observed for specific structures could be understood upon inspection of the transmission electron microscopy (TEM) images of the nanospheres (Figures S1 and S5); these images revealed that the particles were not spherically symmetric, did not have regular shapes, and, most importantly, were not identical, leading to structurally specific interfacial electromagnetic field distributions/orientations and thus to SHG-CD responses that were unique, in both magnitude and sign, for each dimer. The TEM data also indicated the presence of fused SGN dimers (no interparticle gap). Very little SHG intensity was observed for these structures, as they contained only a negligible interparticle gap for field localization and subsequent nonlinear polarizability creation. Furthermore, the SHG-CDR recorded for these samples was significantly dampened relative to that observed for samples characterized by a 1.2 nm interparticle gap, suggesting that interfacial field asymmetry rather than structural symmetry is the dominant contributor to the chirality noted for the SGN dimers. Moreover, observation of a chiral SH response for a majority of the SGN dimers indicated that, in general, the interfacial structures (and the associated interfacial field distribution) were asymmetric in nature. The data shown in Figure 1b clearly demonstrate that collection of unambiguous chiral SHG data for SGN dimers was possible only with single-particle measurements; these data would have been lost by ensemble averaging.

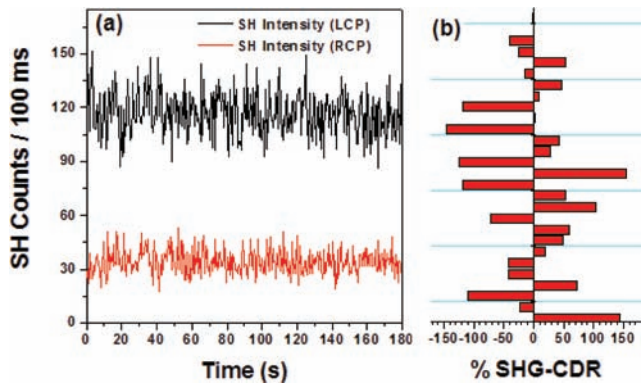

Figure 1. (a) SH intensity traces from a single SGN dimer resulting from LCP and RCP excitation. (b) CDRs measured in the SH response from a number of primitive assemblies of SGNs.

dx.doi.org/10.1021/ja210648a | J. Am. Chem. Soc. 2012, 134, 4477−4480

To demonstrate that the aggregating agent, L-cysteine, was not the source of the CD observed in the SHG signal of the SGN aggregates, the experiments were repeated using SGN dimers anchored together with 1,4-benzenedithiol. This molecule was selected as an aggregating agent because it is achiral and yields a gold−gold interparticle separation distance of ∼1 nm, similar to that found in cysteine-induced dimers. As with the cysteine-induced SGN dimers, the SGNs formed using benzenedithiol exhibited structure-specific chirality in the SHG-CDR, clearly demonstrating the asymmetry in the interfacial field distribution (and not the aggregating agent) to be the main source of the observed chirality. Although this result does not preclude a potential contribution from cysteine to the optical activity of the metal nanostructures it joins, it does indicate that cysteine was not the dominant source of the SHG-CD. The linear CD spectrum of an ensemble of SGN aggregates was also measured. No signature of chirality was seen, although optical activity at the SPR wavelength was recently observed in linear measurements.[33] The absence of optical activity in the linear extinction measured here could be the result of ensemble averaging for heterogeneous aggregates.

To gain deeper insight into the properties of the interfacial fields of SGN dimers, CPV measurements, which can report on the multipolar origin of SHG in any system,[34] were performed. For CPV experiments, the polarization state of the exciting laser beam was varied continuously using a rotating QWP, and the s-polarized SH intensity was recorded as a function of the QWP rotation angle, φ. Measurements were carried out on SGN dimers whose interparticle axes were aligned along the s-polarized direction of the analyzer (see the SI). In general, SHG in any material originates from an induced nonlinear polarization **P** at the fundamental frequency and a magnetization **M** at the harmonic frequency. **P** and **M** are expressed as[34]

$$P_i(2\omega) = \sum_{j,k} \chi_{ijk}^{eee}(2\omega, \omega, \omega)E_j(\omega)E_k(\omega) + \chi_{ijk}^{eem}(2\omega, \omega, \omega)E_j(\omega)B_k(\omega) \quad (2)$$

$$M_i(2\omega) = \sum_{j,k} \chi_{ijk}^{mee}(2\omega, \omega, \omega)E_j(\omega)E_k(\omega) \quad (3)$$

where **E** is the electric field, **B** is the magnetic induction of the incident light, χ is the susceptibility tensor, ω is the carrier frequency of the fundamental wave, and the indices i, j, and k are the Cartesian coordinates of the laboratory frame. Including **P** and **M** as nonlinear sources provides the following general expression for the intensity of the SH field:[34]

$$I(2\omega) = |FE_P^2(\omega) + GE_S^2(\omega) + HE_P(\omega)E_S(\omega)|^2 \quad (4)$$

where $E_P(\omega)$ and $E_S(\omega)$ are the P and S components of the electric field vector of the fundamental field. F, G, and H denote linear combinations of the susceptibility tensors χ^{eee}, χ^{eem}, and χ^{mee} and are generally complex-valued quantities. Of these coefficients, G is the only one that depends exclusively on magnetic-dipole contributions, meaning it must vanish in the electric-dipole approximation. Hence, any nonzero value of G provides a clear signature of magnetic-dipole contributions in the NLO response of a system. This formalism can be modified to reflect an experimentally controllable parameter by expressing E_S and E_P as functions of φ:

$$E_P(\omega) = E_0(\cos^2\varphi + i\sin^2\varphi) = P(\varphi) \quad (5)$$

$$E_S(\omega) = E_0(1 - i)\sin\varphi\cos\varphi = S(\varphi) \quad (6)$$

Using eqs 5 and 6 allows $I(2\omega)$ to be written as[34]

$$I(2\omega) = I(\varphi) = |FP^2(\varphi) + GS^2(\varphi) + HP(\varphi)S(\varphi)|^2 \quad (7)$$

We note that in general, the nonlinear polarization **P** may have a contribution from the electric quadrupole mode that results from retardation effects. This contribution depends strongly on the SH scatterer size and the excitation wavelength.[35−37] In this case, the SH scattering source is confined to the ∼1 nm SGN interparticle gap. Therefore, we assume the 800 nm excitation field to be uniform over the interfacial region, yielding a negligible quadrupolar contribution to the SH field.

The SHG data obtained via the CPV measurements were fit to eq 7 using Igor Pro software to determine the coefficients F, G, and H. Figure 2a,b portrays the experimental CPV data for

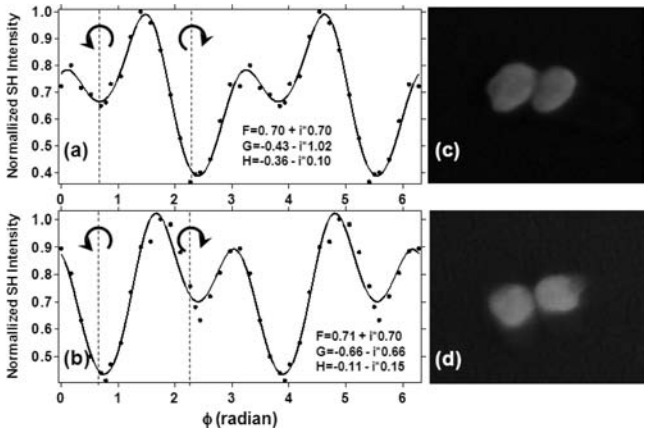

Figure 2. (a, b) SHG line shapes obtained from CPV measurements on two different SGN dimers. Solid dots represent the experimental data, and the solid line is the fit to eq 7. (c, d) SEM images of the dimers whose polarization line shapes are depicted in (a) and (b).

two SGN dimers that were fit to eq 7, and Figure 2c,d shows the corresponding scanning electron microscopy (SEM) images of the dimers. Figure 2a,b immediately reveals that the SH polarization line shapes were asymmetric (i.e., the SH intensity had no parity with respect to φ, corresponding to left and right circular polarizations). The observed asymmetry in the polarization line shapes for SGN dimers provides evidence of the deficiency of the electric-dipole approximation for this system and is a clear indication of the presence of higher-multipole interactions in these nanostructures. Fitting of the experimental data with eq 7 yielded a nonzero value for the coefficient G. In fact, as a result of strong magnetic-dipole interactions between the two particles constituting the SGN dimer, all of the "chiral" SGN dimers studied here yielded nonzero values for the coefficient G. These magnetic dipoles likely gave rise to the observed SHG-CD through interference with the electric dipole, analogous to linear CD. This is, to our knowledge, the first experimental demonstration of magnetic-dipole contributions in the NLO response of bottom-up colloidal metal nanostructure assemblies. Moreover, the magnetic-dipole contribution was evident within the optical frequency range. The observed magnetic-dipole contribution may have originated from the interference of out-of-phase dipole modes. Considering simple structures such as two coupled plasmonic nanospheres (a dimer) and using a hybridization model, antisymmetric resonances would be expected when the excited electric dipoles in the two spheres oscillate 180° out of phase.[38] Such an eigenmode would be strongly subradiant and perceived as a magnetic dipole in

dx.doi.org/10.1021/ja210648a | J. Am. Chem. Soc. 2012, 134, 4477−4480

the far field. Moreover, symmetry breaking in the dimer structure could lead to more oscillator strength in such modes.

Analysis of the CPV measurement data yielded further observations. Similar to the observed structure specificity of the differential SHG in the discrete SGN dimers, the magnetic-dipole contribution to the SHG was also structure-dependent. The values obtained for the parameter G varied significantly among individual SGN dimers (Figure 2; for additional examples, see Figure S5). Detailed tensorial analysis for each individual dimer will be needed to provide a quantitative determination of the exact contribution of each of the multipoles. This information will allow for even deeper insight into the nanostructure-specific symmetry and the details of the electromagnetic fields at the interfaces of bottom-up assemblies.

In conclusion, we have reported the first complete polarization-state analysis of the NLO response of single colloidal plasmonic nanostructures. CD was observed in the SHG signals of individual dimers of gold colloids; most SHG-active dimers exhibited optical activity. This SHG optical activity indicated the presence of an asymmetry within the interfacial field distribution in nanosphere dimers. Single-particle measurements also indicated that the symmetry of these field distributions was highly interfacial-structure-specific. Thorough analysis of the CPV measurements confirmed that the SHG-CD response resulted from strong magnetic-dipole contributions to the electromagnetic coupling of the nanoparticles. This work represents the first experimental observation of magnetic-dipole interactions in the NLO response from colloidal plasmonic nanostructures. The multipolar interactions within the SGN dimers were also shown to be structure-specific. A detailed understanding of these interactions is important for predicting future applications that involve colloidal metal nanoparticles. For example, the field gradients inherent to these nanoparticles could be used as the building blocks for metamaterials and energy up-converting and biosensing devices.

■ ASSOCIATED CONTENT

Ⓢ Supporting Information

Synthetic protocol, experimental layout, TEM images, extinction spectra, and additional CPV-SHG data. This material is available free of charge via the Internet at http://pubs.acs.org.

■ AUTHOR INFORMATION

Corresponding Author

klk@chem.fsu.edu

Notes

The authors declare no competing financial interest.

■ ACKNOWLEDGMENTS

This material is based upon work supported by the U.S. Air Force Office of Scientific Research under AFOSR Award FA9550-10-1-0300 and by ACS PRF 51233-DNI6.

■ REFERENCES

(1) Halas, N. J. *Nano Lett.* **2010**, *10*, 3816.
(2) Eustis, S.; El-Sayed, M. A. *Chem. Soc. Rev.* **2006**, *35*, 209.
(3) Gray, S. K. *Plasmonics* **2007**, *2*, 143.
(4) Ghosh, S. K.; Pal, T. *Chem. Rev.* **2007**, *107*, 4797.
(5) Willets, K. A.; Van Duyne, R. P. *Annu. Rev. Phys. Chem.* **2007**, *58*, 267.
(6) Anker, J. K.; Hall, W. P.; Lyandres, O.; Shah, N. C.; Zhao, J. *Nat. Mater.* **2008**, *7*, 442.
(7) Kabashin, A. V.; Evans, P.; Pastkovsky, S.; Hendren, W.; Wurtz, G. A.; Atkinson, R.; Pollard, R.; Podolskiy, V. A.; Zayats, A. V. *Nat. Mater.* **2009**, *8*, 867.
(8) Law, W. C.; Yong, K. T.; Baev, A.; Hu, R.; Prasad, P. N. *Opt. Express* **2009**, *17*, 19041.
(9) Jackson, J. B.; Halas, N. J. *Proc. Natl. Acad. Sci. U.S.A.* **2004**, *101*, 17930.
(10) Le, F.; Brandl, D. W.; Urzhumov, Y. A.; Wang, H.; Kundu, J.; Halas, N. J.; Aizpurua, J.; Nordlander, P. *ACS Nano* **2008**, *2*, 707.
(11) Camden, J. P.; Dieringer, J.; Zhao, J.; Van Duyne, R. P. *Acc. Chem. Res.* **2008**, *41*, 1653.
(12) Li, J. F.; Huang, Y. F.; Ding, Y.; Yang, Z. L.; Li, S. B.; Zhou, X. S.; Fan, F. R.; Zhang, W.; Zhou, Z. Y.; Wu, D. Y.; Ren, B.; Wang, Z. L.; Tian, Z. Q. *Nature* **2010**, *464*, 392.
(13) Ferry, V. E.; Sweatlock, L. A.; Pacifici, D.; Atwater, H. A. *Nano Lett.* **2008**, *8*, 4391.
(14) Rockstuhl, C.; Lederer, F. *Appl. Phys. Lett.* **2009**, *94*, No. 213102.
(15) Nordlander, P.; Oubre, C.; Prodan, E.; Li, K.; Stockman, M. I. *Nano Lett.* **2004**, *4*, 899.
(16) Aubry, A.; Lei, D. Y.; Maier, S. A.; Pendry, J. B. *ACS Nano* **2011**, *5*, 3293.
(17) (a) Jain, P. K.; El-Sayed, M. A. *Chem. Phys. Lett.* **2010**, *487*, 153. (b) Brown, L. V.; Sobhani, H.; Lassiter, J. B.; Nordlander, P.; Halas, N. J. *ACS Nano* **2010**, *4*, 819.
(18) Fan, J. A.; Bao, K.; Wu, C.; Bao, J.; Bardhan, R.; Halas, N. J.; Manoharan, V. N.; Shvets, G.; Nordlander, P.; Capasso, F. *Nano Lett.* **2010**, *10*, 4680.
(19) Hentschel, M.; Dregely, D.; Vogelgesang, R.; Giessen, H.; Liu, N. *ACS Nano* **2011**, *5*, 2042.
(20) Halas, N. J.; Lal, S.; Chang, W. S.; Link, S.; Nordlander., P. *Chem. Rev.* **2011**, *111*, 3913.
(21) Boyd, R. F. *Nonlinear Optics*; Academic Press: San Diego, 1992.
(22) Canfield, B. K.; Kujala, S.; Laiho, K.; Jefimovs, K.; Turunen, J.; Kauranen, M. *Opt. Express* **2006**, *14*, 950.
(23) Kujala, S.; Canfield, B. K.; Kauranen, M.; Svirko, Y.; Turunen, J. *Opt. Express* **2008**, *16*, 17196.
(24) Kujala, S.; Canfield, B. K.; Kauranen, M.; Svirko, Y.; Turunen, J. *Phys. Rev. Lett.* **2007**, *98*, No. 167403.
(25) Husu, H.; Canfield, B. K.; Laukkanen, J.; Bai, B.; Kuittinen, M.; Turunen, J.; Kauranen, M. *Appl. Phys. Lett.* **2008**, *93*, No. 183115.
(26) Husu, H.; Canfield, B. K.; Laukkanen, J.; Bai, B.; Kuittinen, M.; Turunen, J.; Kauranen, M. *Metamaterials* **2008**, *2*, 155.
(27) Valev, V. K.; Smisdom, N.; Silhanek, A. V.; Clercq, B. D.; Gillijns, W.; Ameloot, M.; Moschalkov, V. V.; Verbiest, T. *Nano Lett.* **2009**, *9*, 3945.
(28) Palomba, S.; Danckwerts, M.; Novotny, L. *J. Opt. A* **2009**, *11*, No. 114030.
(29) Corn, R. M.; Higgins, D. A. *Chem. Rev.* **1994**, *94*, 107.
(30) Fan, J. A.; Wu, C.; Bao, K.; Bardhan, R.; Halas, N. J.; Manoharan, V. N.; Nordlander, P.; Shvets, G.; Capasso, F. *Science* **2010**, *328*, 1135.
(31) Ghosh, S. K.; Pal, A.; Kundu, S.; Nath, S.; Pal, T. *Chem. Phys. Lett.* **2004**, *395*, 366.
(32) Chandra, M.; Dowgiallo, A. M.; Knappenberger, K. L. Jr. *J. Am. Chem. Soc.* **2010**, *132*, 15782.
(33) Slocik, J. M.; Govorov, A. O.; Naik, R. R. *Nano Lett.* **2011**, *11*, 701.
(34) Kauranen, M.; Verbiest, T.; Persoons, A. *J. Mod. Opt.* **1998**, *45*, 403.
(35) Nappa, J.; Revillod, G.; Russier-Antoine, I.; Benichou, E.; Jonin, C.; Brevet, P. F. *Phys. Rev. B* **2005**, *71*, No. 165407.
(36) Russier-Antoine, I.; Benichou, E.; Bachelier, G.; Jonin, C.; Brevet, P. F. *J. Phys. Chem. C* **2007**, *111*, 9044.
(37) Chandra, M.; Das, P. K. *Chem. Phys.* **2009**, *358*, 203.
(38) Riikonen, S.; Romero, I.; Garca de Abajo, F. J. *Phys. Rev. B* **2005**, *71*, No. 235104.